Original Article

Image processing and machine learning approach for yolk color evaluation

Supreeya Thepparak[1] Chusak Pulmar[2] Chanwit Kaewtapee[1*]

Abstract

The objective of this study was to develop a predictive model for yolk color measurement using machine learning. A total of eight hundred eggs were randomly collected from thirty laying hens (Lohmann brown, 28–35 weeks). The experimental diets were formulated based on broken rice or corn and further supplemented with canthaxanthin from 10 to 150 mg/kg. The Digital YolkFan™ was used to classify yolk color scales from 0 to 15, whereas the Hunter Lab was used to measure color values. Furthermore, yolk images were obtained from a digital camera and then extracted into red color, green color and blue (RGB) and hue, saturation and value (HSV). Machine learning, including multiple linear regression, decision tree (DT), support vector machine, artificial neural networks and deep learning were used to develop the predictive models. The accuracy of R^2 was greater for the HSV (0.971) than for the Hunter Lab (0.969) and RGB (0.947) approaches. The root mean square error (RMSE) was also lower for HSV than for Hunter Lab and RGB (0.770, 0.805 and 1.055, respectively). Further improvement based on HSV with DT achieved the highest accuracy (R^2 = 0.996) and the lowest statistical error measurements (RMSE = 0.288). In conclusion, the HSV obtained from the digital yolk image provided a suitable color system, with the use of the DT model expected to improve the accuracy of prediction. Therefore, combined digital imagery and machine learning provided a rapid and highly cost-effective technique requiring little human subjectivity for yolk color evaluation.

Keywords: Decision tree, digital image, laying hen, machine learning, yolk color

[1]*Department of Animal Science, Faculty of Agriculture, Kasetsart University, Bangkok 10900, Thailand*

[2]*Department of Animal Science, Faculty of Agricultural Technology and Agro-industry, Rajamangala University of Technology Suvarnabhumi, Phra Nakhon Si Ayutthaya 13000, Thailand*

***Correspondence**: agrcwk@ku.ac.th* (C. Kaewtapee)

Received March 27, 2023

Accepted May 14, 2023

https://doi.org/10.14456/tjvm.2023.11

Introduction

Egg yolk color is a determining factor in a consumer's decision to purchase eggs. Globally, the preference for yolk color may vary, such as being golden-yellow to orange in the USA and reddish in the EU and Asia, corresponding to values on the Roche Yolk Color Fan® scale in the ranges 5–10 and 11–14, respectively (Galobart *et al*., 2004; Hisasaga *et al*., 2020). The yolk color is generally affected by diet supplementation with carotenoids, such as lutein and canthaxanthin. The measurement of yolk color can be determined individually by visual perception (Vuilleumier, 1969). However, the color scale might be perceived differently depending on personal perception (Dvořák *et al*., 2009), resulting in variation in the color scale scoring between observers. In view of this drawback, instruments, such as spectrophotometers have been developed to measure color values, which are represented as lightness (*L**), redness (*a**) and yellowness (*b**) and have been used for evaluating yolk color (Dvořák *et al*., 2009) and heated soybean quality (Kaewtapee *et al*., 2017). Recently, a color sensor, known as the Digital YolkFan™ has been introduced to ensure consistent yolk color measurements for egg producers (Nix Sensor Ltd., 2022).

In computer vision, color images can be extracted and then transformed into digital data as red, green and blue (RGB) or hue, saturation and value (HSV). For image analysis, RGB is the most common color system based on the linear function of three numerical components in the range 0–255 (Russ, 2005; Łuszczkiewicz-Piątek, 2014). In contrast, the HSV color system involves a nonlinear transformation of RGB color, which allows for a computer-based interpretation of color values similar to human perception, in the ranges 0–360 for hue and 0–100 for saturation and value (Hamuda *et al*., 2017). The RGB color approach has been used as a color index for the estimation of the chlorophyll content in quinoa and amaranth leaves (Riccardi *et al*., 2014) and the prediction of the nitrogen content in rice (Qiu *et al*., 2021). Likewise, the HSV color system has been applied for the identification of greenness in maize seeding images (Yang *et al*., 2015) and discrimination among cauliflower plants (Hamuda *et al*., 2017).

Machine learning (ML) is a subset of artificial intelligence and consists of several models, such as multiple linear regression (MLR), decision tree (DT), support vector machines (SVM), artificial neural networks (ANN) and deep learning (DL; Liakos *et al*., 2018). Regarding color assessment, the MLR model with *L**, *a** and *b** has been used to evaluate meat quality (O'Sullivan *et al*., 2003) and the SVM model with RGB color has been used to detect rice disease (Chung *et al*., 2016), while the DT model with HSV color has identified maize seedings under different conditions (Yang *et al*., 2015) and discriminated crop, weed and soil in the field (Hamuda *et al*., 2017). Furthermore, ANN and DL models using RGB or HSV colors have evaluated tomato quality in the ripening stage (Moreira *et al*., 2022). However, no published information is available on yolk color evaluation using a digital image. Therefore, the objective of this study was to compare different color systems and to develop predictive models using ML for yolk color measurement.

Materials and Methods

Ethical approval: The research proposal was reviewed and approved by the Animal Care and Use for Scientific Research Committee, Kasetsart University (Bangkok, Thailand), and Care of animals throughout this experiment was in accordance with the corresponding Ethical Principles for the use of animals for scientific purposes according to National Research Council of Thailand (1999; Approval Number: ACKU64-AGR-023).

Animals and general management: A total of 30 laying hens (Lohmann brown, 28–35 weeks) were used. Each bird was kept in an individual cage with a wire mesh floor (40 cm wide × 40 cm deep × 30 cm high) and equipped with a feeding trough and nipple drinker. The temperature in the experimental unit was maintained at 25°C using an automated evaporative cooling system. The daily lighting period comprised 16 h. Water and feed were offered *ad libitum* throughout the experimental period.

Experimental diets: The control diet, based on broken rice, soybean meal and full-fat soybeans, was formulated to meet nutrient recommendations of Lohmann Brown-classic layers (17% protein, 2,725 kcal/kg; Table 1). The control diet was supplemented with corn at the levels of 0, 5, 10, 15, 20, 25, 30, 35, 40, 45 and 50% at the expense of broken rice. The assay diet based on 50% of corn was further supplemented with canthaxanthin pigment (Leader®, Foshan Leader Bio-Technology Co. Ltd., Foshan, China) at the levels of 10, 20, 30, 50, 70, 90 and 150 mg/kg.

Color measurement: The experimental design was completely randomized in 4 periods with 6 treatments and 5 replications. In each period, laying hens were allowed to adapt to the assay diets for 7 days and then eggs were collected continuously from days 8 to 14 for determining yolk color and egg quality. In total, 800 egg yolks determined a color scale using a Digital YolkFan™ (Nix™, Nix Sensor Ltd., Ontario, Canada), ranging from very light yellow (scale 0) through orange to red (scale 15). In addition, Hunter Lab (Spectrophotometer MiniScan EZ, Hunter Associates Laboratory Inc., Virginia, USA) was also used to measure the yolk color, represented as *L**, *a** and *b** values.

Image acquisition and image processing: The eight hundred yolk images were obtained from a digital camera (Sony Cyber-Shot DSC W830, Sony Group Corporation, Japan) with a resolution of 5152 × 3864 pixels. The digital images were taken using a mini-photography box (14.9 cm wide × 14.9 cm deep × 14.9 cm high) with a light-emitting diode. The image processing technique was coded using Python in the Google Colaboratory (Google, California, USA). Briefly, the image was uploaded into the program where the yolk area was detected for its yellow-orange color and marked by a red square. Five positions (1, top; 2, left; 3, middle; 4, right and 5, below) from the center of the yolk area were used to extract the color values as RGB values and HSV values (Figure 1). The data was split 80:20 for training and testing datasets, respectively. The training dataset (640 yolk images) was used for the development of the ML model, while the testing dataset (160 yolk images) was used to validate the performance of the obtained model.

Table 1 Feed ingredients and chemical composition of the control diet[1] (g/kg, as fed-basis).

Ingredients	Amount (%)
Broken rice	50.00
Soybean meal (44% protein)	24.72
Full fat soybean	10.00
Limestone	9.90
Monocalcium phosphate	1.80
Vitamin and mineral premix[2]	0.25
Sodium bicarbonate	0.40
Salt	0.30
Soybean oil	2.40
DL-methionine	0.23
Pigment	-
Total	100.00
Nutrient content (calculated)	
Metabolizable energy (kcal/kg)	2,787
Total protein (%)	18.73
Ash (%)	2.72
Fat (%)	6.79
Neutral detergent fiber (%)	9.66
Acid detergent fiber (%)	4.30
Total Calcium (%)	4.12
Available Phosphorus (%)	0.43
Lysine (%)	1.02
Methionine (%)	0.51
Methionine + Cystine (%)	0.81

[1]Assay diets were obtained by adding corn at levels of 0, 5, 10, 15, 20, 25, 30, 35, 40, 45, and 50% to the basal diet at the expense of broken rice.

[2]Vitamin and mineral premix content (per kg of diet): vitamin A 10,000 IU, vitamin D3 2,500 IU, vitamin E 5 IU, vitamin K3 2 mg, vitamin B1 1 mg, vitamin B2 3 mg, vitamin B6 3 mg, vitamin B12 20 µg, pantothenic acid 4.5 mg, niacin 20 mg, folic acid 0.5 mg, biotin 0.01 mg, choline chloride 125 mg, selenium 0.15 mg, iron 50 mg, manganese 77.5 mg, zinc 50 mg, copper 4 mg, cobalt 1 mg, iodine 1 mg, calcium carbonate 925 mg, preservative 1.4 mg.

Machine learning models: The RGB and HSV color values obtained from the digital yolk images were used to develop the ML models as follows:

The MLR model is a well-known approach for developing a relationship between the dependent variable (Y) and more than one independent variable (X) for the best fit straight line as follows:

$$Y_i=\beta_0+\beta_1X_1+\beta_2X_2+\ldots+\beta_kX_k+\varepsilon$$

where Y_i is the predicted value of the dependent variable, β_0 is the y-intercept, β_1, β_2, ..., β_k are the coefficients of independent variables (X_1,X_2 ..., X_k) and ε is the model error.

DT is a classification or regression model formulated like a tree architecture. Each internal node of the tree structure represents a different pairwise comparison on a selected feature, whereas each branch represents the outcome of this comparison and leaf nodes represent the final decision or prediction taken after following the path from the root to the leaf (Belson *et al.*, 1959; Liakos *et al.*, 2018). The model is shown below:

$$P=-\sum_{i=0}^{k}\frac{freq(C_i,P)}{|P|}\log_2\left(\frac{freq(C_i,P)}{|P|}\right)$$

where P is entropy and if P is any collection of samples, then (C_i, P) is the overall number of samples in P that belong to C_i, and |P| is the number of samples in P.

The SVM model involves differentiation of the decision margin, which contains the greatest distance from the nearest training data points in any setting. This algorithm model can achieve a strong separation and the classifier has a greater margin and a lower error (Pedregosa *et al.*, 2011). The function of SVM is shown below:

$$f(x)=\omega\psi(x)+b$$

where ω is the weights, b is the offset degree and $\psi(x)$ is the nonlinear mapping.

An ANN is based on the biological neuron of the human brain responding to an optimal predictive value (Sivanandam *et al.*, 2006). The architecture consists of three layers: (1) an input layer, where the data is fed into the system (color values); (2) a hidden layer, where the learning takes place; and (3) an output layer, where the decision or the prediction takes place (McCulloch *et al.*, 1943; Liakos *et al.*, 2018). The hyperbolic tangent function and the linear activation function are used in the hidden and output layers, respectively. The functions are computed as

Hyperbolic tangent:

$$f(x) = \frac{e^{x} - e^{-x}}{e^{x} + e^{-x}},$$

Linear activation:

$$f(x) = x,$$

where x represents the weighted sum of inputs to the neuron and f(x) indicates the outputs from the neuron.

Finally, DL can be classified as a subset of ANN containing several hidden layers (Han *et al*., 2011). In the present study, the full DL was designed in three hidden layers with 300 nodes each. The rectified linear unit (ReLU) was used as the activation function in each layer. The ReLU function is shown as:

$$f(x) = \max(0, x),$$

where x represents the weighted sum of inputs and f(x) is the corresponding output from neurons. There were 1,000 training epochs and 0.0001 learning rates. The Adam solver was used as an optimization tool that can handle sparse gradients, requires limited memory capacity and is well suited for a large dataset or large parameters.

Statistical analysis: Data on egg quality was statistically analyzed by ANOVA of SAS (SAS® Studio, SAS Institute Inc., North Carolina, United States). Results were presented as mean ± standard deviation. Differences between treatments were assessed using Tukey's Studentized Range test. Statistical significance was considered at $P < 0.05$. The prediction equations for yolk color measurement were developed using MLR, DT, SVM, ANN and DL with the scikit-learn library (BSD License, France). Correlation coefficients (r) were determined between the yolk color scale and color values using the CORR procedure of SAS. The accuracy of each predictive model was determined based on the coefficient of multiple determination (R^2), whereas the statistical error measurements were calculated based on the root mean square error (RMSE) and mean absolute error (MAE), according to principles described by Kaewtapee *et al*. (2011).

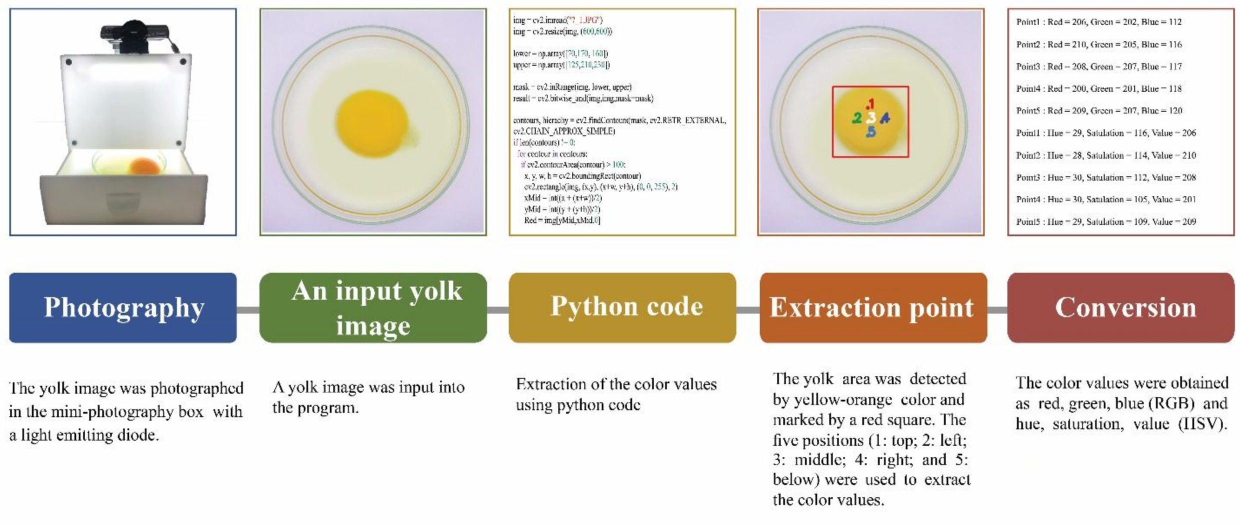

Figure 1 Flow chart of the image processing technique to obtain yolk color values.

Table 2 Correlation between the yolk color scale (Digital YolkFan™) and color values.[1]

Correlation coefficient (r)	Yolk color scale (Digital YolkFan™)	*L**	*a**	*b**	Red	Green	Blue	Hue	Saturation
*L**	-0.947								
*a**	0.982	-0.957							
*b**	0.403	-0.298	0.326						
Red	0.802	-0.779	0.835	0.129					
Green	-0.864	0.852	-0.867	-0.299	-0.507				
Blue	-0.635	0.612	-0.585	-0.584	-0.221	0.681			
Hue	-0.942	0.905	-0.951	-0.308	-0.809	0.832	0.478		
Saturation	0.748	-0.717	0.703	0.601	0.385	-0.734	-0.982	-0.608	
Value	0.799	-0.775	0.831	0.128	0.998	-0.500	-0.214	-0.805	0.378

*L**=Lightness, *a**=Redness, *b**=Yellowness.
[1]All values were statistically significant at $P < 0.05$.

Results

Egg quality: The yolk color of laying hens fed the different levels of corn and CXT is presented in Figure 2. The results show that the yolk color scale increased ($P < 0.05$) from 1 to 7 as the supplementation of corn was from 5 to 30% but no significant difference was observed in the yolk color scale between 7 and 8 when the corn was supplemented in the diet between 30 and 50%. The yolk color was further increased from a scale 9 to 15 as the CXT was included in the diet from 10 to

150 mg/kg. However, there were no significant differences ($P > 0.05$) in egg quality among all groups.

Color values: The correlations determined between the yolk color scale and color values are presented in Table 2. The yolk color scale showed a high positive correlation ($P < 0.05$) with a^* (r = 0.982) and a high negative correlation ($P < 0.05$) with L^* (r = -0.947). With regard to RGB, the yolk color scale had a high negative correlation ($P < 0.05$) with green (r = -0.864) and a high positive correlation ($P < 0.05$) with red (r = 0.802). For HSV, the yolk color scale had a high negative correlation ($P < 0.05$) with hue (r = -0.942) and a moderate positive correlation (P < 0.05) with saturation (r = 0.748) and value (r = 0.799).

The coefficient of multiple determination and statistical error measurements of the MLR models are presented in Table 3. The accuracy of the MLR model using HSV was higher than for Hunter Lab and RGB, respectively. Likewise, the error measurements were lowest in the MLR model using HSV compared to Hunter Lab and RGB, respectively. The MLR models were shown as follows:

Yolk color scale = 6.930 - 0.725Hue + 0.047Saturation + 0.044Value ($R^2 = 0.971$)

Yolk color scale = 2.662 - 0.070L^* + 0.370a^* + 0.065b^* ($R^2 = 0.969$)

Yolk color scale = -7.542 + 0.189Red - 0.122Green - 0.048Blue ($R^2 = 0.947$))

The scatter plot and histogram between the yolk color scale and color values are presented in Figure 3. The results showed that the yolk color scale increased as L* decreased and as a* and b* increased for the Hunter Lab system, with greater red and lower green and blue for RGB and lower hue and greater saturation and value for HSV.

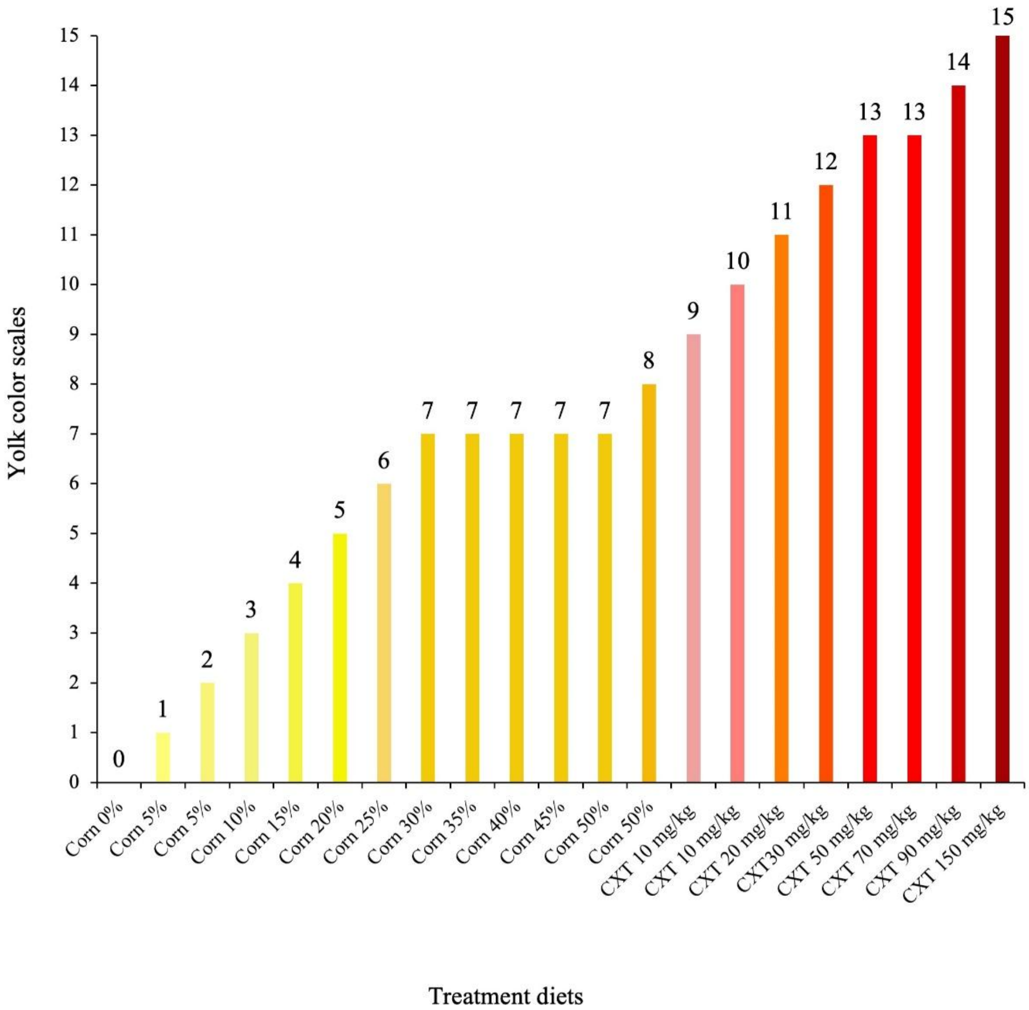

Figure 2 Yolk color scale with different levels of corn and canthaxanthin (CXT) levels in laying hen diets.

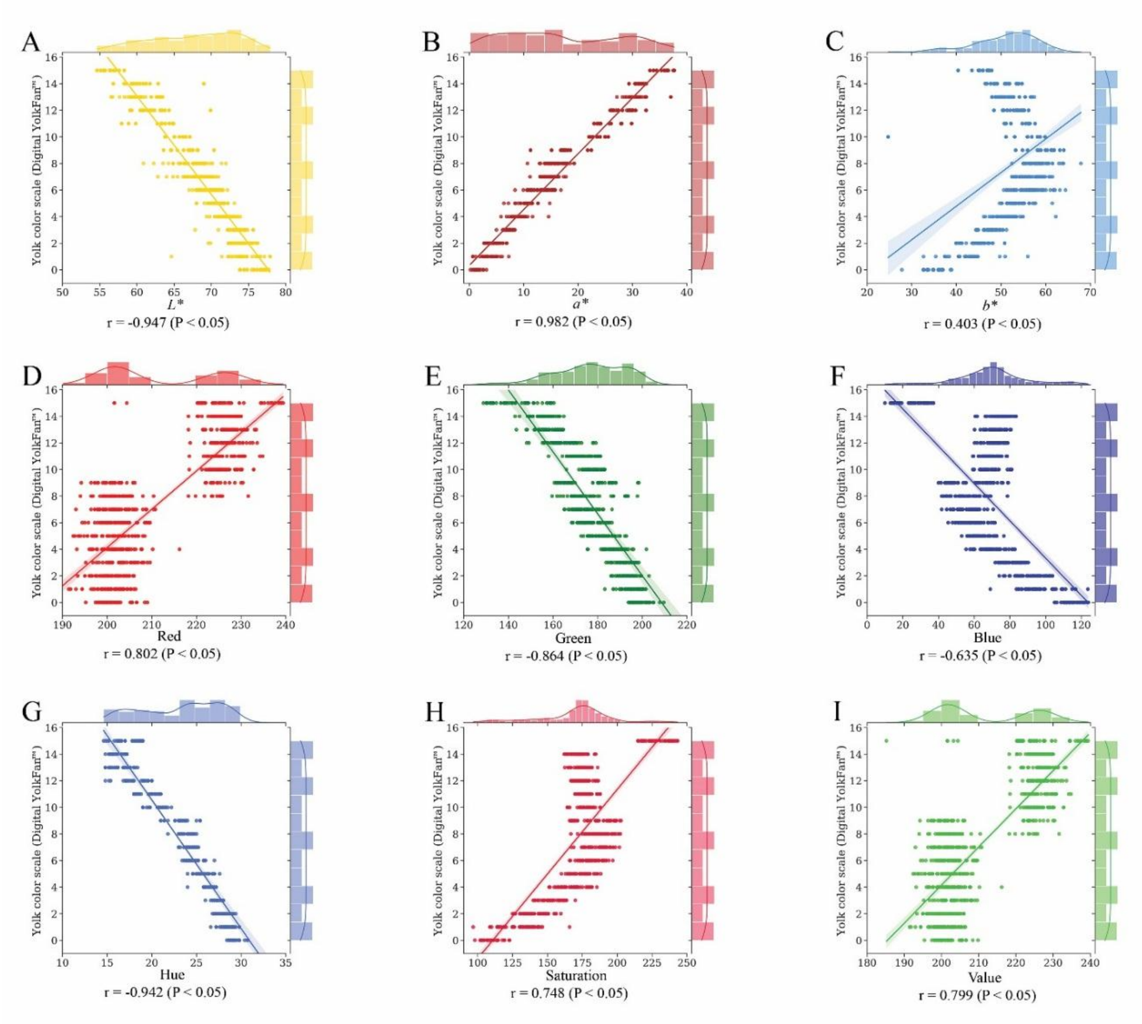

Figure 3 Scatter plot, histogram and correlation coefficient (r) between yolk color scale and color values: (A) *L**, (B) *a**, (C) *b**, (D) red, (E) green, (F) blue, (G) hue, (H) saturation and (I) value.

Table 3 Coefficient of multiple determination (R^2) and statistical error measurements of yolk color scale based on multiple regression analysis.

Data	Statistical parameter	Hunter Lab (*L**, *a** and *b**)	Digital image	
			RGB	HSV
Training dataset (n = 640)	R^2	0.969	0.947	0.971
	RMSE	0.805	1.055	0.770
	MAE	0.527	0.688	0.505
Testing dataset (n = 160)	R^2	0.966	0.940	0.967
	RMSE	0.848	1.127	0.833
	MAE	0.531	0.705	0.531

*L**=Lightness, *a**=Redness, *b**=Yellowness, R=Red, G=Green, B=Blue, H=Hue, S=Saturation, V=Value, RMSE=Root mean square error, MAE=Mean absolute error.

Table 4 Coefficient of multiple determination (R^2) and statistical error measurements of yolk color scale using machine learning model with HSV color.

Data	Statistical parameter	Machine learning			
		DT	SVM	ANN	DL
Training dataset (n = 640)	R^2	0.996	0.956	0.971	0.974
	RMSE	0.288	0.971	0.780	0.743
	MAE	0.080	0.613	0.495	0.455
Testing dataset (n = 160)	R^2	0.996	0.943	0.968	0.971
	RMSE	0.296	1.098	0.829	0.766
	MAE	0.088	0.694	0.519	0.450

H=Hue, S=Saturation, V=Value, DT=Decision tree, SVM=Support vector machine, ANN=Artificial neural networks, DL=Deep learning, RMSE=Root mean square error, MAE=Mean absolute error.

Machine learning models: The coefficient of multiple determination and statistical error measurements of the predictive models, including HSV, are presented in Table 4. Greater accuracy and lower statistical error in the training and testing datasets were observed in DT compared to DL, ANN and SVM, respectively.

Discussion

Lutein and zeaxanthin are known as xanthophyll carotenoids, which are presented as yellow or orange color in fruits and vegetables (Ortiz *et al*., 2022). The pigments in corn are also classified as xanthophyll carotenoids and the higher levels of corn in the diet can increase the accumulation of yellow color in egg yolk (Rowan, 1989). In the present study, the supplementation of corn from 0 to 30% in the diet increased yolk color scales up to 7. The yolk color remained scale 7 with the supplementation of corn between 30 and 50%, indicating the saturation of xanthophyll carotenoids. Furthermore, the red color of egg yolk can be achieved by the supplementation of CXT. This is in agreement with the study of Sandeski *et al*. (2014), where adding CXT in laying hen diets resulted in a reddish-orange yolk color scale up to 14. Notably, the supplementation of either corn or broken rice had no effect on production performance and egg quality. Similarly, the increasing levels of broken rice from 0 to 100% in quail diets did not affect feed intake, body weight gain and feed conversion ratio (Filgueira *et al*., 2014) the same as the replacement of corn at the expense of wheat or barley resulted in no differences in feed intake and egg quality (Lázaro *et al*., 2003).

Spectrophotometers have been used to accurately measure yolk color and to reduce the reliance on subjective human appraisal, based on values for L^*, a^* and b^* (Dvořák *et al*., 2009). The results from the present study were in line with Grashorn and Steinberg (2002), where a greater value on the yolk color scale meant a decreasing L^* and an increasing a^*. Interestingly, RGB is the most common color value scale used, as it can be used as a rapid method for color measurement (Russ, 2005). With regard to plantations, RGB was used to evaluate the chlorophyll content in quinoa and amaranth leaves, with the results producing better accuracy and a lower error of prediction than from a leaf chlorophyll meter (Riccardi *et al*., 2014). Furthermore, an RGB image provided a color value for monitoring the nitrogen content in rice (Qiu *et al*., 2021). However, the use of RGB is sometimes limited due to the lack of differentiation based on color intensity and illumination (Riehle *et al*., 2020). Alternatively, HSV is a nonlinear transformation of RGB, which is represented as hue (red, yellow, green and blue or a combination of these colors), saturation (the intensity of the color) and value (more or less light); therefore, it has been suggested that HSV is more related to human perception than RGB (Łuszczkiewicz-Piątek *et al*., 2014; Hamuda *et al*., 2017). Furthermore, the conversion of RGB to HSV for crop images avoided the influence of illumination, resulting in improved greenness identification for crop growth (Yang *et al*., 2015). This was supported by the present study, where HSV produced higher precision than RGB. One possible reason was that the international standard scale of yolk color is based on human perception. Therefore, HSV seemed to be more reliable for evaluating the color quality of egg yolk.

For color assessment of animal products, advanced instruments have been developed with a light-sensing device to determine the color value based on the reflectance and transmission of light and are represented as L^*, a^* and b^* values (Hunter and Harold, 1987). Furthermore, the determination of L^*, a^* and b^* values is a more precise method for yolk color measurement than human evaluation (Dvořák *et al*., 2009). However, the instrument is expensive and has a high maintenance cost. In the present study, HSV provided higher accuracy and lower error in the predictive model compared to Hunter Lab. Therefore, HSV data obtained from a digital image can be considered as a cost-effective method to measure yolk color with improved accuracy compared to current techniques.

For precision animal agriculture, ML has been used to develop models for genomic prediction (Long *et al*., 2007) and pig weight estimation (Kaewtapee *et al*., 2019). Among ML models, the DT model with HSV correctly recognized greenness in maize seed (Yang *et al*., 2015) and was highly sensitive to cauliflower crop discrimination (Hamuda *et al*., 2017). Similar findings were reported in the present study, where the DT model with HSV effectively improved the yolk color, perhaps because the DT model was gradationally learned using a small subset, from which a decision diagram was generated with connected tree leaves (Belson *et al*., 1959). However, the low precision levels of the other models (SVM, ANN and DT) may have been due to the overlapping values between neighboring points on the yolk color scale, resulting in the poor performance of the SVM (Sarker, 2021), as was the case for the ANN and DL approaches (Balabin and Lomakina, 2011). Therefore, DT provided the best-fitting model that could be used to estimate the yolk color with high accuracy.

In conclusion, the yolk color increased up to scale 7 with the levels of corn in laying hen diets between 30 and 50%. However, the supplementation of either corn or broken rice had no significant differences in production performance and egg quality. The color values based on HSV obtained from a digital image could be used to develop a DT model of yolk color quality, which resulted in high accuracy and lower error measurements compared to other ML models. Therefore, digital images and machine learning can be combined to provide a rapid method with reducing human subjectivity for yolk color evaluation.

Conflicts of interest: All authors certify that there is no conflict of interest.

Acknowledgements

This research is funded by Kasetsart University through the Graduate School Fellowship Program.

References

Balabin RM and Lomakina EI 2011. Support vector machine regression (SVR/LS-SVM)—an alternative to neural networks (ANN) for analytical chemistry? Comparison of nonlinear methods on near infrared (NIR) spectroscopy data. Analyst. 136: 1703–1712.

Belson WA 1959. Matching and prediction on the principle of biological classification. J R Stat Soc Ser C Appl Stat. 8: 65–75.

Chowdhury SD, Hassin BM, Das SC, Rashid MH and Ferdaus AJM 2008. Evaluation of marigold flower and orange skin as sources of xanthophyll pigment for the improvement of egg yolk color. J Poult Sci. 45: 265–272.

Chung CL, Huang KJ, Chen SY, Lai MH, Chen YC and Kuo YF 2016. Detecting Bakanae disease in rice seedlings by machine vision. Comput Electron Agric. 121: 404–411.

Dvořák P, Doležalová J and Suchý P 2009. Photocolorimetric determination of yolk colour in relation to selected quality parameters of eggs. J Sci Food Agric. 89: 1886–1889.

Galobart J, Sala R, Rincón-Carruyo X, Manzanilla EG, Vilà B and Gasa J 2004. Egg yolk color as affected by saponification of different natural pigmenting sources. J Appl Poult Res. 13: 328–334.

Filgueira TMB, Freitas ER, Filho IBQ, Fernandes DR, Watanabe PH and Oliveira AN 2014. Corn replacement by broken rice in meat-type quail diets. Braz J Poult Sci. 16: 345–350.

Grashorn MA and Steinberg W 2002. Deposition rates of canthaxanthin in egg yolks. Arch Geflügelk. 66: 258–262.

Hamuda E, Ginley BM, Glavin M and Jones E. 2017. Automatic crop detection under field conditions using the HSV colour space and morphological operations. Comput Electron Agric. 133: 97–107.

Han J, Kamber M and Pei J 2011. Data mining: concepts and techniques. 3rd ed. Morgan Kaufmann Publishers is an imprint of Elsevier. 703 pp.

Hisasaga C, Shinn SE and Tarrant KJ 2020. Survey of egg quality in commercially available table eggs. Poult Sci. 99: 72029–77206.

Hunter RS and Harold RW 1987. The measurement of appearance. 2nd ed. John Wiley and Sons. 432 pp.

Kaewtapee C, Khetchaturat C and Bunchasak C 2011. Comparison of growth models between artificial neural networks and nonlinear regression analysis in Cherry Valley ducks. J Appl Poult Res. 20: 421–428.

Kaewtapee C, Eklund M, Wiltafsky M, Piepho H-P, Mosenthin R and Rosenfelder P 2017. Influence of wet heating and autoclaving on chemical composition and standardized ileal crude protein and amino acid digestibility in full-fat soybeans for pigs. J Anim Sci. 95: 779–788.

Kaewtapee C, Rakangtong C and Bunchasak C 2019. Pig weight estimation using image processing and artificial neural networks. J Adv Agric Technol. 6: 253–256.

Lázaro R, García M, Araníbar MJ and Mateos GG 2003. Effect of enzyme addition to wheat, barley and rye based diets on nutrient digestibility and performance of laying hens. Br Poult Sci. 44: 256–265.

Liakos KG, Busato P, Moshou D, Pearson S and Bochtis D 2018. Machine learning in agriculture: a review. Sensors. 18: 2674.

Long N, Gianola D, Rosa GJM, Weigel KA and Avendano S 2007. Machine learning classification procedure for selecting SNPs in genomic selection: application to early mortality in broilers. J Anim Breed Genet. 124: 377–389.

Łuszczkiewicz-Piątek M 2014. Which color space should be chosen for robust color image retrieval based on mixture modeling. Adv Intell Syst Comput. 233: 55–64.

McCulloch WS and Pitts W 1943. A logical calculus of the ideas immanent in nervous activity. Bull Math Biophys. 5: 115–133.

Moreira G, Magalhães SA, Pinho T and Santos FN. 2022. Benchmark of deep learning and a proposed HSV colour space models for the detection and classification of greenhouse tomato. Agronomy. 12: 356–378.

Nix Sensor Ltd. 2022. “Digital YolkFan™.” [Online]. Available: https://www.dsm.com/anh/products-and-services/tools/digital-yolkfan.html. Accessed February 20, 2022.

Ortiz D, Lawson T, Jarrett R, Ring A, Scoles KL, Hoverman L, Rocheford E, Karcher DM and Rocheford T 2022. Applied Research Note: “The impact of orange corn in laying hen diets on yolk pigmentation and xanthophyll carotenoid concentrations on a percent inclusion rate basis”. J Appl Poult Res. 31: 100218.

O’SullivanMG, Byrne DV, Martens H, Gidskehaug LH, Andersen HJ and Martens M 2003. Evaluation of pork colour: prediction of visual sensory quality of meat from instrumental and computer vision methods of colour analysis. Meat Sci. 65: 909–918.

Qiu Z, Ma F, Lia Z, Xua X, Gea H and Du C 2021. Estimation of nitrogen nutrition index in rice from UAV RGB images coupled with machine learning algorithms. Comput Electron Agric. 189: 106421.

Riccardi M, Mele G, Pulvento C, Lavini A, d'Andria R and Jacobsen SE 2014. Non-destructive evaluation of chlorophyll content in quinoa and amaranth leaves by simple and multiple regression analysis of RGB image components. Photosynth Res. 120: 263–272.

Riehle D, Reiser D and Griepentrog HW 2020. Robust index-based semantic plant/background segmentation for RGB-images. Comput Electron Agric. 169: 105201.

Rowan KS 1989. Photosynthetic Pigments of Algae. 1st ed. Cambridge University Press. 350 pp.

Russ JC 2005. Image analysis of food microstructure. 1st ed. CRC Publisher. 384 pp.

Sandeski LM, Ponsano EH and Neto MG 2014. Optimizing xanthophyll concentrations in diets to obtain well-pigmented yolks. J Appl Poult Res. 23: 409–417.

Sarker IH 2021. Machine learning: Algorithms, real-world applications and research directions. SN Comput Sci. 2: 1–21.

Sivanandam SN, Sumathi A and Deepa SN 2006. Introduction to neural networks using Matlab 6.0. 1st ed. Tata McGraw-Hill Publishers Company Limited. 656 pp.

Vuilleumier JP 1969. The 'Roche yolk colour fan'—An instrument for measuring yolk colour. Poult Sci. 48: 767–779.

Yang W, Wang S, Zhao X, Zhang J and Feng J 2015. Greenness identification based on HSV decision tree. Inf Process Agric. 2: 149–160.